2017

Detecting pulsars in the Galactic Centre

K. M. Rajwade

D. R. Lorimer

L. D. Anderson

Mon. Not. R. Astron. Soc. **000**, 1–?? (2002) Printed 29 June 2017 (MN LaTeX style file v2.2)

Detecting pulsars in the Galactic centre

K. M. Rajwade[1,2⋆], D. R. Lorimer[1,2,3] and L. D. Anderson[1,2,3]
1. Department of Physics and Astronomy, West Virginia University, Morgantown, WV 26506, USA
2. Center for Gravitational Waves and Cosmology, West Virginia University, Chestnut Ridge Research Building, Morgantown, WV 26505, USA
3. Green Bank Observatory, Green Bank, WV 24944, USA

29 June 2017

ABSTRACT
Although high-sensitivity surveys have revealed a number of highly dispersed pulsars in the inner Galaxy, none have so far been found in the Galactic centre (GC) region, which we define to be within a projected distance of 1 pc from Sgr A*. This null result is surprising given that several independent lines of evidence predict a sizable population of neutron stars in the region. Here, we present a detailed analysis of both the canonical and millisecond pulsar populations in the GC and consider free-free absorption and multi-path scattering to be the two main sources of flux density mitigation. We demonstrate that the sensitivity limits of previous surveys are not sufficient to detect GC pulsar population, and investigate the optimum observing frequency for future surveys. Depending on the degree of scattering and free-free absorption in the GC, current surveys constrain the size of the potentially observable population (i.e. those beaming towards us) to be up to 52 canonical pulsars and 10000 millisecond pulsars. We find that the optimum frequency for future surveys is in the range of 9–13 GHz. We also predict that future deeper surveys with the Square Kilometer array will probe a significant portion of the existing radio pulsar population in the GC.

Key words: Pulsars:general — Galaxy:centre — scattering — radiative transfer.

1 INTRODUCTION

Understanding the stellar populations in the Galactic centre (GC) region, and how they relate to the central supermassive black hole (Sgr A*), is a major goal of modern astrophysics. The central few parsecs of the Galaxy are known to consist of large molecular complexes and have high stellar densities compared to the rest of the Galactic disk (see, e.g., Schödel et al. 2007). Under these circumstances, many authors have already made the reasonable assumption that a large population of neutron stars exist in the GC (Morris & Serabyn 1996; Genzel et al. 2010).

Motivated by the promise of finding pulsars orbiting Sgr A*, there have been multiple surveys of the GC region (Johnston et al. 2006; Macquart et al. 2010; Deneva 2010; Bates et al. 2011). These surveys are typically conducted at frequencies higher than ∼1 GHz to reduce the impact of interstellar scattering, which is known to cause potentially significant pulse broadening along lines of sight to pulsars in the inner Galaxy (Cordes & Lazio 1997). To date, no pulsars have been found in the GC region which we define in this paper to be within 1 pc of Sgr A* (i.e. an angular offset of 25″ for $R_0 = 8.3$ kpc). The discovery of a magnetar (Eatough et al. 2013; Mori et al. 2013) has brought the problem of pulsars in the GC to fore again. The discovery led Chennamangalam & Lorimer (2014) and Dexter & O'Leary (2014) to conclude that there are very few pulsars in the GC. Moreover, Dexter & O'Leary (2014) also go on to suggest that the magnetar formation efficiency is higher in the GC and the lack of detection could be attributed to shorter life spans of magnetars. These results seem puzzling, given the high stellar density of the GC. Also, angular broadening measurements of SGR 1745−2900 have revealed that the scattering along this line of sight is less than expected. Bower et al. (2014) claim that the scattering screen along the line of sight lies ∼ 6 kpc away from the GC in the Scutum arm. These findings suggest that previous surveys should have discovered more pulsars in the GC, which makes their dearth baffling.

The presence of hot, ionized gas in the central parsec of our Galaxy (Pedlar et al. 1989; Gillessen et al. 2012) raises the question of whether absorption can affect detection of radio pulsars. Recent studies have shown free-free thermal absorption to be the primary source of gigahertz peaked spectra, where the flux density spectrum shows a turnover at frequencies of ∼1 GHz in some pulsars found in dense ionized environments (Lewandowski et al. 2015; Rajwade et al. 2016). The GC environment suggests that absorption by ionized gas could decrease the observed flux density from neutron stars beaming towards us.

⋆ kmrajwade@mix.wvu.edu

Such a dense and highly turbulent environment can also be responsible for large scattering, thereby, reducing incoming pulsar radio flux density in our line of sight. The effects of the interstellar medium (ISM) in the GC on pulsar flux densities have been studied previously. Cordes & Lazio (1997) modeled multi-path scattering in the GC in terms of a thin screen near the centre. As a result, the radio pulses observed can be substantially broadened at lower frequencies. Wharton et al. (2012) studied various flux density mitigation effects due to the ISM that can alter the incoming pulsar flux and result in a non-detection. Recently, Macquart & Kanekar (2015) proposed that the neutron star population of the GC is dominated by millisecond pulsars (MSPs). They also claimed that more sensitive, high frequency surveys in the future would be able to detect MSPs in the GC. Though a MSP population has been predicted in the past, the results of Macquart & Kanekar (2015) are based on the pseudo-luminosity distribution of known pulsar population sample, which has an inherent pseudo-luminosity bias since we only detect the brightest pulsars.

In this paper, we try to answer questions regarding the GC pulsar population by modeling the GC environment and accounting for observational selection biases. We simulate a pulsar population in the GC environment and study the effect of the GC environment on pulsar flux densities. We find the optimum frequency for future surveys based on the results of the simulation. Section 2 describes the simulations with different models considered. In Section 3, we present the results of the analysis and their implications.

2 SIMULATIONS

To place constraints on the number of pulsars in the GC, we simulated synthetic populations of pulsars using the PsrPopPy package (Bates et al. 2014), a python module based on the `psrpop` code developed earlier for population synthesis of pulsars (Lorimer et al. 2006). The inferred parameters from the known pulsar population in the Galaxy are biased due to various selection effects (see, e.g., Faucher-Giguère & Kaspi 2006). These effects are accounted for by PsrPopPy (see Bates et al. 2014, for details). PsrPopPy generates synthetic pulsar populations based on a set of pulsar parameters. These are then searched for in a simulated pulsar survey based on past survey parameters to determine the subset of pulsars, that are theoretically detectable.

We considered populations of canonical pulsars (CPs) and millisecond pulsars (MSPs) in our analysis with PsrPopPy (Bates et al. 2014). For both cases, we simulated the populations using the pseudo-luminosity scaling with period and period derivative. Following previous authors, we parametrize the pseudo-luminosity L in terms of period P and period derivative $\dot{P}$ as a power law:

$$L = \gamma P^{\alpha} \dot{P}^{\beta}, \tag{1}$$

where α, β and γ are model parameters. For simplicity, following Bates et al. (2014), we take $\alpha = -1.4$ and $\beta = 0.5$ which physically links L to be proportional to the square root of the pulsar's spin-down pseudo-luminosity. The uncertainties on α and β are reported in Bates et al. (2014). To ensure that errors on α and β do not affect our results, we reran our simulations by changing one parameter by 1σ and kept the other same. We observed that changing the parameters within the errors had little to no effect on the results as discussed later. To ensure that the properties of the simulated sample are comparable to the observed sample, we modified the constant of proportionality in this expression, γ so that the pseudo-luminosity of the simulated sample that is detected in a simulated Parkes survey matches the observed detected sample in the same survey, assuming that the properties of the pulsars in the GC are similar to the properties of detected pulsars. To achieve this, we simulated a population of CPs and MSPs for different γs and ran a Kolmogorov-Smirnov (K-S) test on the pseudo-luminosity distributions of the simulated and the observed sample for both sub-populations. Since the K-S probability beyond ~ 0.1 implies that the model and observed distributions are statistically indistinguishable (see, e.g., Press et al. 2002), we obtain a range of γ values for which the luminosities are consistent as shown in Fig. **??**. The best γ was chosen for the case where we obtained the maximum K-S probability for the two detected populations. The best simulated populations were used for further analysis. The parameters used for simulation of both populations are given in Table 1. We note in passing here that the optimal values of γ found here imply population-averaged luminosity values of 2.1 mJy kpc^2 and 0.1 mJy kpc^2 for CPs and MSPs respectively. Although our analysis does not make any distinction between solitary and binary MSPs which appear to have different luminosities (Bailes et al. 1997; Burgay et al. 2013), it does clearly show that MSPs are intrinsically fainter radio sources than CPs.

We scaled the derived luminosities of the simulated population at 1.4 GHz to different frequencies given in Table 4 for both populations assuming a normal distribution of spectral indices (Bates et al. 2013). Then, the corresponding observed flux density

$$S = \frac{L_{\nu}}{D_{\rm GC}^2}, \tag{2}$$

where L_{ν} is the pseudo-luminosity at a frequency ν (see Chennamangalam & Lorimer 2014, for details) and $D_{\rm GC}$ is the distance to the GC which is assumed to be 8.3 kpc (Bower et al. 2014).

We obtained flux densities for different frequencies from luminosities obtained in the simulations using Eq. 2. Then, using the models discussed in the subsequent sections, we multiplied the flux densities by the appropriate factors to account for the reduction due to three scenarios: (i) Scattering, where the flux density is reduced due to multi-path scattering between the source and the observer; (ii) Free Free absorption, where the radio flux density from the pulsar is absorbed by the intervening medium; (iii) Both scattering and free-free absorption playing a role in flux density mitigation. Under these circumstances, we calculated the upper limit on CP and MSP populations for previous and future surveys. For a given model, survey and a sample size, we ran multiple realizations of our simulations and we repeated the same experiment for a range of sample sizes of the GC pulsar population. Then, we counted the number of times our simulations produce no detection for a given sample size. This exercise enabled us to generate a probability density function (PDF) of these null results as a function of sample size. To compute the 95% confidence level upper limit on

Parameter	CP	MSP
Radial distribution Model	Lorimer et al. (2006)	Lorimer et al. (2006)
Initial Galactic z-scale height	50 pc	50 pc
1-D velocity dispersion	265 km s^{-1}	80 km s^{-1}
Maximum initial age	1 Gyr	5 Gyr
Luminosity parameter α	-1.4 (1)	-1.4 (1)
Luminosity parameter β	0.50 (4)	0.50 (4)
Luminosity parameter γ	0.35	0.009
Spectral index Distribution	Gaussian	Gaussian
$\langle\alpha\rangle$	-1.4	-1.4
σ_α	0.9	0.9
Initial Spin period distribution	Gaussian	Log-Normal (Lorimer et al. 2015)
$\langle P\rangle$ (ms)	300	—
σ_P (ms)	150	—
$\langle\log_{10}\mathrm{P(ms)}\rangle$	—	15
$std(\log_{10}\mathrm{P(ms)})$	—	56
Pulsar spin-down model	Faucher-Giguère & Kaspi (2006)	Faucher-Giguère & Kaspi (2006)
Beam alignment model	orthogonal	orthogonal
Braking Index	3.0	3.0
Initial B-field distribution	Log-normal	Log-normal
$\langle\log_{10}\mathrm{B(G)}\rangle$	12	8
$std(\log_{10}\mathrm{B(G)})$	0.55	0.55
Observed sample size	1065	39

Table 1. Table showing the different model parameters used in PsrPopPy for simulation of the two pulsar populations. The values used in the simulation are adopted from previous Parkes surveys (Manchester et al. 2001; Edwards et al. 2001). Values in the parenthesis indicate 1-σ uncertainties on the least significant digit.

Survey	Frequency	T_{sys}	t_{int}	G	S/N_{min}	$\Delta\nu$
	(GHz)	(K)	(s)	(K Jy^{-1})		(MHz)
Bates et al. 2011	6.5	40	1055	0.6	10	576
Macquart et al. 2010	15	35	21600	1.5	10	800
Johnston et al. 2006	8.4	40	4200	0.6	10	864
SKA-MID	5	30	50400	17.7	10	770
ngVLA	10	34	25200	22.4	10	8000

Table 2. Basic parameters for previous and future pulsar surveys towards the GC.

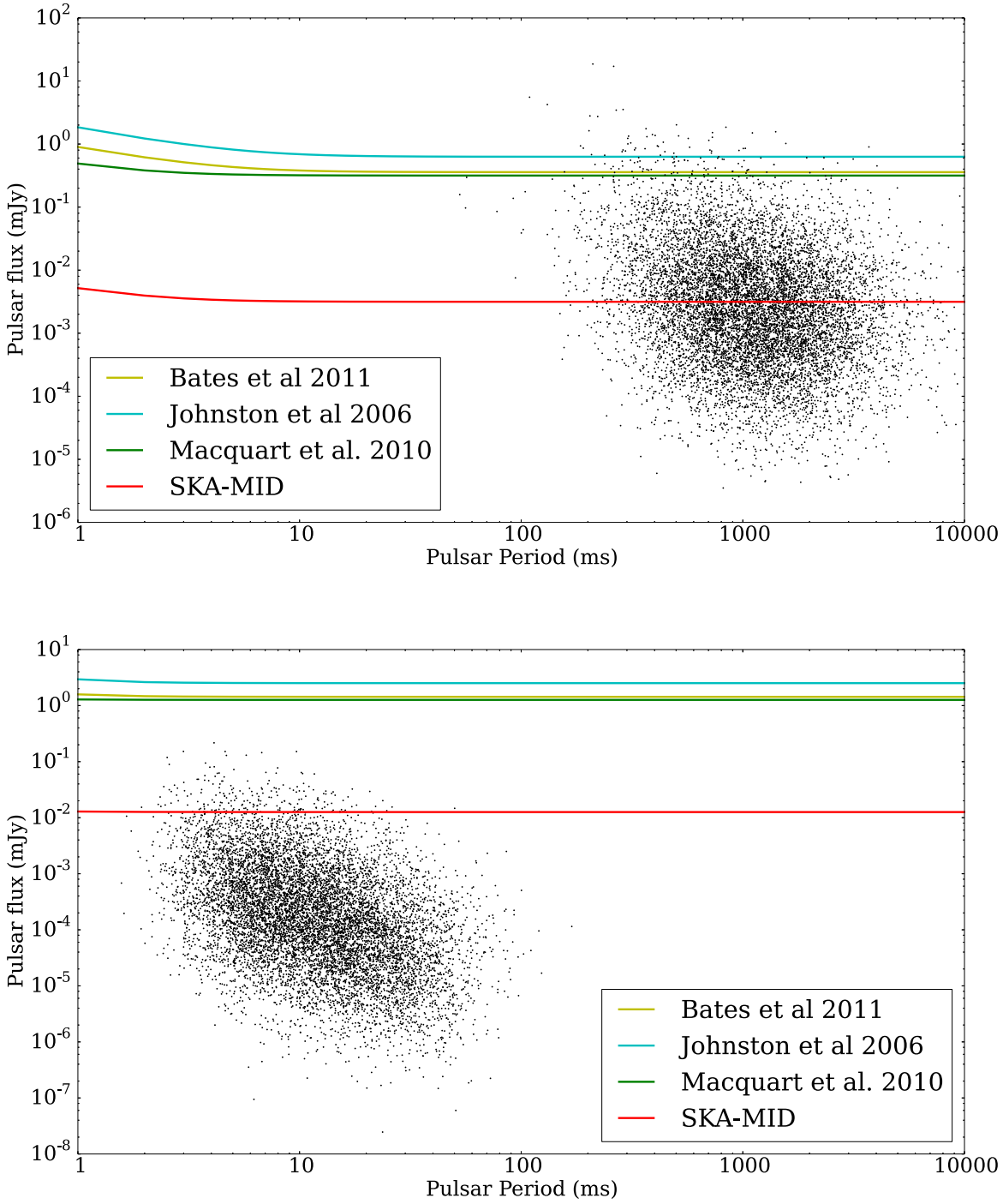

Figure 1. 1.4 GHz mean flux density versus period for a synthetic population of 10000 pulsars at the GC for the baseline model (BL). The top panel shows CPs while the bottom panel shows MSPs. Different lines indicate the survey sensitivities of past surveys apart from the SKA-MID survey. The parameters for SKA-MID survey are the expected parameters of the telescope. The sensitivities of each survey have been scaled to 1.4 GHz assuming a spectral index of –1.4 (Bates et al. 2013). The flux density limit curves for each survey correspond to a DM of 1780 cm^{-3} pc. The flux sensitivity limit for ngVLA is not shown since it almost overlaps with the SKA-MID flux limit.

Model	Survey									
	A		B		C		D		E	
	CP	MSP	CP	MSP	CP	MSP	CP	MSP	CP	MSP
BL	353	4840	444	5200	130	820	11	38	10	27
WS	354	4950	444	5775	130	830	11	44	10	27
SS	375	–	445	–	130	1020	13	–	10	350
FF	353	4900	444	5700	130	820	11	41	10	27
FF+WS	360	5585	444	5800	130	830	12	44	10	27
FF+SS	378	–	445	–	130	1020	13	–	10	350

Table 3. Table showing 95% confidence level upper limits on the population for a null result in previous and future surveys. These are conservative limits since we use the lowest acceptable γ values. The surveys considered here are: (A) Bates et al. (2011); (B) Johnston et al. (2006); (C) Macquart et al. (2010); (D) SKA-MID survey; (E) ngVLA survey. The models listed are: (1) the baseline (BL) model with no scattering or free-free absorption; (2) weak scattering (WS); (3) strong scattering (SS); (4) free-free absorption (FF); (5) free-free and weak scattering (FF+WS); (6) free-free and strong scattering (FF+SS).

the CP and MSP populations, we calculated the sample size such that the area under the PDF was 0.95 times the total area under the curve. For this analysis, where we report conservative limits on the GC pulsar populations, we used the lowest γ value above a K-S probability of 0.1. Since the change in α and β within 1σ errorbars affected the number of detected pulsars in a given survey by a factor of $\sim$1, we conclude that the change in those parameters does not affect our upper limits. The results of this analysis are shown in Table 3. Figure. 1 shows the baseline simulation of CPs and MSPs with past survey sensitivities overlaid along with future SKA-MID and ngVLA (Carilli et al. 2015) survey with assumed parameters of the telescope [1]. The results of the past surveys along with the ngVLA and SKA-MID survey are shown in Table 3. From this it is evident that, even without considering any effects of the GC environment on the pulsar flux densities, the past surveys have been insensitive to the total pulsar population in the GC.

2.1 Model

In an attempt to make sense of the lack of pulsars in the GC found so far, we developed a model described below that takes account of multi-path scattering and free-free absorption effects on the pulsar signal. If S_0 is the intrinsic flux density of a pulsar at a frequency ν, then the measured flux density at the telescope

$$S_\nu = S_{0,\nu}\ \mathcal{S}(\nu)\ \mathcal{F}(\nu), \tag{3}$$

where $\mathcal{S}(\nu)$ and $\mathcal{F}(\nu)$ are the flux density mitigation factors due to scattering and free-free absorption respectively. These factors are discussed in turn in the sections below.

2.1.1 Free-Free absorption

Free-free absorption is known to bias flux density spectra of some pulsars (Lewandowski et al. 2015; Rajwade et al. 2016). This is manifested by a turnover in pulsar spectra at frequencies of $\sim$1 GHz (Kijak et al. 2007, 2011) which is different from the turnover seen at lower frequencies due to synchrotron self absorption (Sieber 1973). This phenomenon is normally observed in pulsars that lie in dense environments like pulsar wind nebulae or supernova remnants. Since the GC consists of dense, ionized gas and cold molecular gas with thin ionization fronts, we assume free-free absorption plays a part in reducing the flux density of an expected pulsar population at the GC. If τ is the optical depth along a given line of sight then, as we showed in Rajwade et al. (2016), the observed flux density

$$S_{\mathrm{obs},\nu} = S_{\mathrm{ref},\nu_{\mathrm{ref}}}\ \left(\frac{\nu}{\nu_{\mathrm{ref}}}\right)^{\alpha}\ \mathcal{F}(\nu), \tag{4}$$

where

$$\mathcal{F}(\nu) = \exp\left[-\tau_\nu \left(\frac{\nu}{\nu_{\mathrm{ref}}}\right)^{-2.1}\right], \tag{5}$$

and $S_{\mathrm{ref},\nu_{\mathrm{ref}}}$ is the pulsar's observed flux density at a reference frequency ν_{ref} at which $\tau_\nu \ll 1$. For a correction factor of order unity[2], the optical depth

$$\tau_\nu = 0.082 \left(\frac{\nu}{\mathrm{GHz}}\right)^{-2.1} \left(\frac{\mathrm{EM}}{\mathrm{cm^{-6}\ pc}}\right) \left(\frac{T_e}{\mathrm{K}}\right)^{-1.35}. \tag{6}$$

For this analysis, following Pedlar et al. (1989), we adopt an emission measure EM = $5{\times}10^5$ cm^{-3} pc and electron temperature T_e= 5000 K for the GC. Rajwade et al. (2016) shows that this effect is smaller at frequencies greater than $\sim$1 GHz, which will be discussed later.

2.1.2 Scattering

Given a flux density spectrum that is modified by free-free absorption in the GC region, we also need to consider the impact of multi-path scattering. Observations of scatter-broadened pulse profiles, which are typically in the form of a one-sided exponential, have long been known to be powerful probes of the physical composition and structure of the ISM (for a review, see e.g., Krishnakumar et al. 2015). Since the GC is a region with high stellar density and large amounts of molecular and ionized gas, a significant amount of scattering is expected for pulsars in this region. From Cordes & Lazio

[1] `https://www.skatelescope.org/wp-content/uploads/2012/07/SKA-TEL-SKO-DD-001-1_BaselineDesign1.pdf`

[2] This assumption is reasonable so long as $T_e > 20$ K, which is the case in this work.

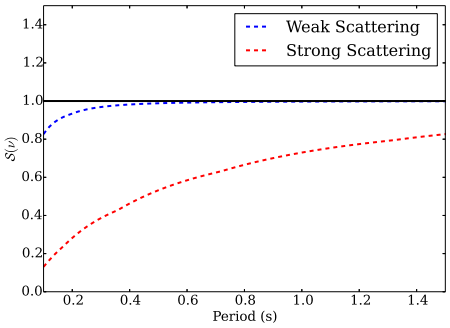

Figure 2. Scattering efficiency ($\mathcal{S}(\nu)$) as a function of period for CPs. The horizontal black line corresponds to $\mathcal{S}(\nu) = 1$.

(1997), for observations at some frequency ν and scattering due to a thin screen, the corresponding scattering timescale

$$t_{\rm sca}(\Delta_{\rm GC}) = 6.3{\rm s} \left(\frac{D_{\rm GC}}{8.5\ {\rm kpc}}\right) \left(\frac{\theta_{\rm GC,1\ GHz}}{1.3''}\right)^2 \left(\frac{\nu}{\rm GHz}\right)^{-4} \left(\frac{D_{\rm GC}}{\Delta_{\rm GC}}\right) \left(1 - \frac{\Delta_{\rm GC}}{D_{\rm GC}}\right). \quad (7)$$

In this expression, $D_{\rm GC}$ is the distance to the GC, $\Delta_{\rm GC}$ is the distance of the scattering screen from the GC and $\theta_{\rm GC}$ is the angular broadening of Sgr A* scaled to a frequency of 1 GHz. We compute $\mathcal{S}(\nu)$ following the treatment in Cordes & Lazio (1997) and Cordes & Chernoff (1997). We assume pulses to be characterized by a Gaussian and convolve this with a one-sided exponential scattering function to broaden the pulse. In Fourier space, the amplitude of the harmonics will be the product of the Fourier transform of the Gaussian pulse and the scattering function. Since the scattering reduces the peak amplitude of the pulse, that manifests itself as a reduction in the efficiency of the survey. We define this efficiency

$$\mathcal{S}(\nu) = \frac{\eta_{\rm p,sc}}{\eta_{\rm p,std}}, \quad (8)$$

where $\eta_{p,sc}$ is the pulsed fraction for the scattered pulse and $\eta_{p,std}$ is the pulsed fraction of the standard Gaussian pulse (See Appendix A for details). The position of the scattering screen towards the GC is still uncertain. For this analysis, we assume strong scattering scenario with the screen at ∼130 pc (Cordes & Lazio 1997) and weak scattering with screen at ∼6 kpc from the GC (Bower et al. 2014). We did these calculations for CPs and MSPs for weak and strong scattering. Figure 2 shows the efficiency as a function of period for CPs. For this analysis, we used a constant duty cycle of 0.4 for MSPs and 0.05 for CPs.

2.2 Probability of detection

Finally, we computed a probability of detecting a single pulsar (CP and MSP) at the GC as a function of frequency and screen distance for each of the three scenarios (scattering, free-free absorption and both effects) by considering surveys of the GC with the Green Bank Telescope (GBT). We selected the GBT because it is one of the largest fully steerable single dish telescope where one can observe the GC for a significant duration. We adopted the known parameters of Green Bank Telescope (GBT) receivers from the GBT observing guide[3] to compute the flux density limit at different frequencies for future GBT surveys (see Table 4). The sky contribution from the GC to the system temperature is significant and since the GC transits at an elevation of ∼21°, it was necessary to account for the changes in the system temperature, $T_{\rm sys}$ at lower elevations. To do this we assumed, the system temperature of each receiver,

$$T_{\rm sys} = T_{\rm GC} + T_{\rm atm} + T_{\rm rec}, \quad (9)$$

where, $T_{\rm GC}$ is the contribution of the GC, $T_{\rm atm}$ is the contribution due to the atmosphere and $T_{\rm rec}$ is the constant receiver temperature. $T_{\rm GC}$ is computed by taking the weighted average of $T_{\rm GC}(\nu)$ over the band of the receiver. To compute $T_{\rm GC}(\nu)$, we used the recent continuum maps of the GC at 1.4, 6 and 9.2 GHz from Law et al. (2008). Using the calibrated maps, we used the flux density at the pixel coresponding to the GC to fit a power-law which led to a relationship

$$T_{\rm GC}(\nu) = 568 \left(\frac{\nu}{\rm GHz}\right)^{-1.13} {\rm K}. \quad (10)$$

For $T_{\rm atm}$, we computed empirical relations between $T_{\rm atm}$ and elevation for each receiver which made use of data from the GBT sensitivity calculator [4]. Then, we computed the weighted average of $T_{\rm atm}$ over all hour angles of the source by taking into account the dependence of elevation with hour angle. The final $T_{\rm sys}$ is calculated by plugging in values for $T_{\rm GC}$, $T_{\rm atm}$ and $T_{\rm rec}$ in Eq. 9. The final values of flux density sensitivities are given in Table 4 For multi-beam receivers, we assumed only a single beam. In these calculations, we are not assuming any coherent summing of multiple epochs. Using the flux densities computed in the simulation, we obtained flux density histograms of the synthesized population at different GBT frequencies and counted up the number of the pulsars above the flux density threshold of each survey. The required detection probability is simply the ratio of pulsars above each survey threshold to the total number of pulsars simulated.

In 2012, a new backend was developed for the GBT. The VErsatile GBT Astronomical Spectrometer (VEGAS) is currently being used observations (Bussa & VEGAS Development Team 2012). The backend consists of 8 different spectrometer banks and has a maximum total instantaneous bandwidth of 1250 MHz for pulsar observations. VEGAS is expected to be the primary backend for pulsar astronomy and will replace the Green Bank Ultimate Pulsar Processing Instrument (GUPPI) (Ransom et al. 2009) in the process. Hence, in our analysis, we assume VEGAS to be the primary backend for future GBT pulsar surveys. Under these assumptions, we computed probability of detection for two scenarios: (a) the backend would be able to accommodate the entire bandwidth of each receiver; (b) using VEGAS as the backend in which case the bandwidth is limited to 1250 MHz. The 2-D histograms for both the cases are shown in Fig. 3 and Fig. 4.

[3] https://science.nrao.edu/facilities/gbt/proposing/GBTpg.pdf
[4] https://dss.gb.nrao.edu/calculator-ui/war/Calculator_ui.html

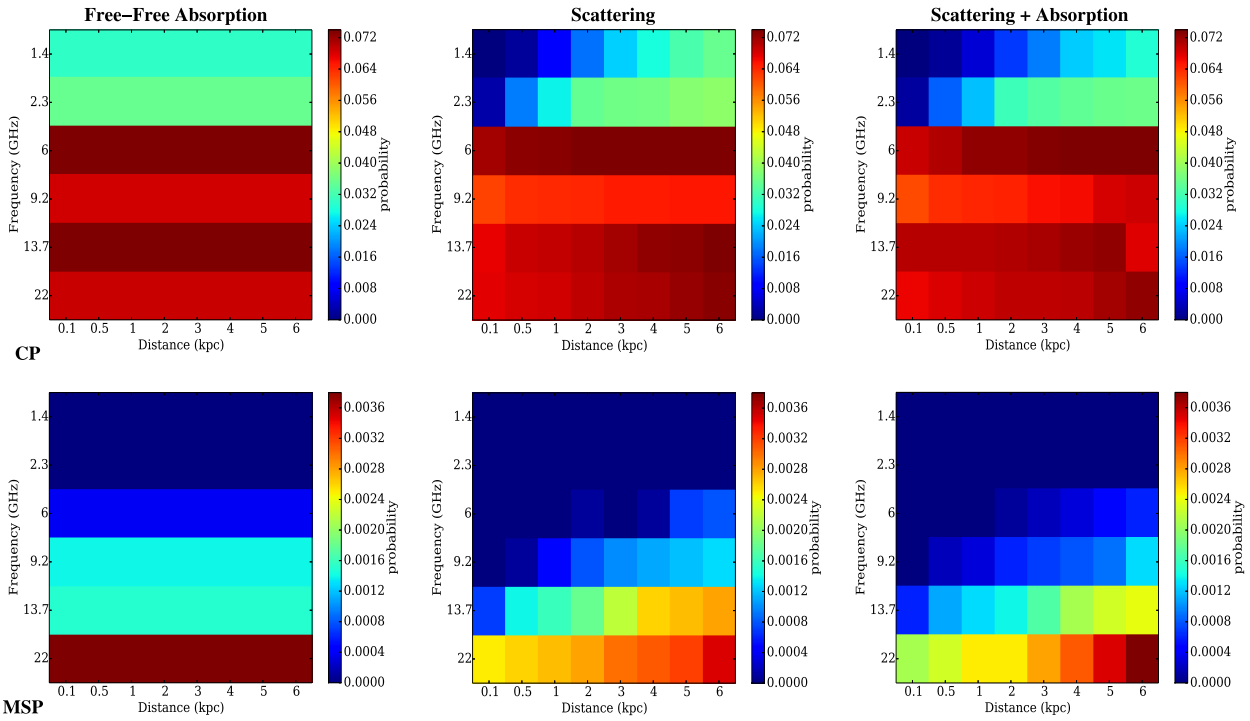

Figure 3. Probability of finding a pulsar in the GC as function of frequency and distance of the scattering screen from the GC in future GBT surveys assuming that the backend would be able to incorporate the whole bandwidth of each receiver. The columns from left to right are: free-free absorption, scattering, both scattering and absorption. The upper row is for CPs while the bottom one is for MSPs.

Receiver	Central Frequency	Bandwidth	10-σ Sensitivity Limit	VEGAS Limit	Detection probabilities expressed as percentages			
					Future backends		VEGAS	
	(GHz)	(MHz)	μJy	μJy	CP	MSP	CP	MSP
L-Band	1.4	650	119	119	$\leqslant 3.5$	0.0	$\leqslant 3.5$	0.0
S-Band	2.3	970	62.3	62.3	$\leqslant 3.9$	0.0	$\leqslant 3.9$	0.0
C-Band	6	3800	12.2	20.3	8	0.08	5.3	$\leqslant 0.04$
X-Band	9.2	2400	11.3	16.3	7	0.14	5.2	0.05–0.09
Ku-Band	13.7	3500	8.4	14.0	7.5	0.2–0.3	5.3	0.1
KFPA	22	8000	6.7	17.3	7.3	0.9–1.3	0.4	0.1–0.2

Table 4. Table showing various parameters of the GBT receivers with corresponding survey limit for a future survey of the GC (see text for details). The details for receivers are given in `https://science.nrao.edu/facilities/gbt/facilities/gbt/proposing/GBTpg.pdf`.

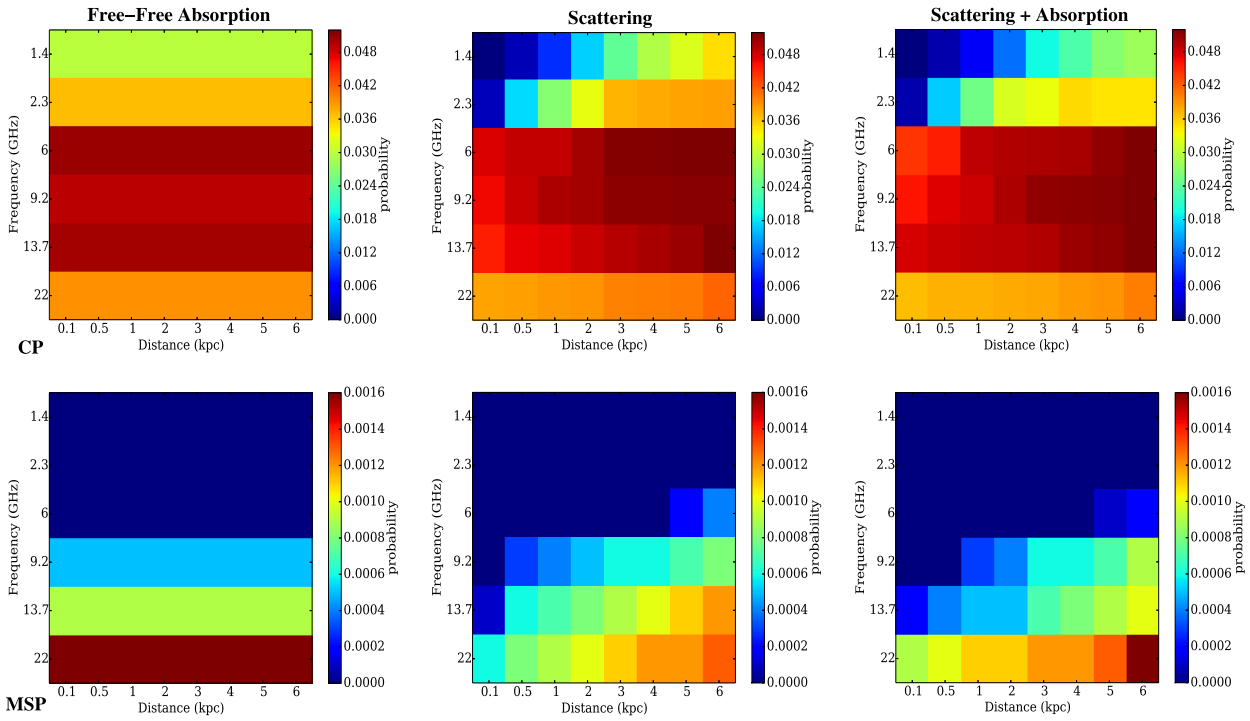

Figure 4. Probability of finding a pulsar in the GC as function of frequency and distance of the scattering screen from the GC. The probabilities have been computed for future GBT surveys and assuming VEGAS as the backend. The banding seen in the free-free absorption case is due to the different bandwidths of receivers on the GBT.

2.3 Results

Tables 3 and 4 clearly summarize our results from the analysis mentioned above. Table 3 shows the upper limits on the populations based on previous and future surveys for various models. The results point out that based on the null results from previous surveys, we can obtain an upper limit on the CP and MSP population in the GC and the results do not reject an existence of CP population in the GC. With the expected performance of SKA-MID and ngVLA, we would be able to probe a sizable population of GC pulsars which would give us much better constraints. The constraints on the pulsar population are less stringent as we include models for flux density mitigation as we would detect a lesser fraction of the existing population due to the effects of the ISM. Table 4 summarizes probabilities of finding one pulsar in a potential GBT survey. Results show that CPs have a better prospect of being detected than MSPs though the absolute probability is only as high as 0.07. Moreover, Table 3 suggests that current observations are less constraining on the MSP population than the CP population. The small number of predicted CPs would suggest that star formation is suppressed at the GC and that the existence of MSPs could be explained through capture of MSPs from globular cluster (Hooper & Linden 2016).

3 DISCUSSION

Although the probability of detecting a single pulsar is greater than zero for higher frequencies, where scattering and absorption effects are negligible, the value itself is small. This can be attributed to the distance of the GC where the flux densities of pulsars in the GC would be so small that even without assuming any attenuation of the flux density, we have been able to probe only a small fraction of the population. Irrespective of the dominance of sub populations in the GC (CP or MSP), the faintness of these sources due to the distance of the GC makes it difficult to detect them. This is clearly indicated by Fig. 1 where the survey sensitivity limit only encloses $0-2\%$ of the total simulated population of CPs and 0% of the total MSP population for the baseline model. This shows that we need deeper searches of the GC in the future even if the environment does not play a role in affecting pulsar flux densities. Our results allow for $\sim$ 445 CPs beaming towards us which is a less constraining compared to the results in Chennamangalam & Lorimer (2014) by a factor of 2. We also obtain an upper limit of 5800 MSPs in the GC which is far less constraining compared to the CPs. Chennamangalam & Lorimer (2014) take into account the magnetar population as a magnetar fraction in the GC and their results suggest previous surveys were not sensitive to existing pulsar population in the GC. Dexter & O'Leary (2014) suggest that given the absence of hyper-strong scattering and lack of pulsar detections, there might be an intrinsic deficit of pulsars in the GC though our simulations suggest our radio surveys have not been sensitive enough to detect any pulsars in the GC. The detection of one magnetar hints at a preference to creation of magnetars in the GC. Future SKA and ngVLA surveys will be able to answer these questions.

Figs. 3 and 4 show the probability of detection for different frequencies and screen distances for MSPs and CPs. The figures show that free-free absorption has negligible ef-

fect on the flux density mitigation beyond frequencies of 1 GHz due to negligible optical depths at higher frequencies. Hence, the probability of detection is solely dependent on the bandwidth of the telescope receivers. The banding structure evident in the figure is due to the fact that different GBT receivers have different bandwidths. On the other hand, scattering plays an important role in reducing flux density from pulsars. Scattering transitions from strong scattering to weak scattering regime as the distance of the screen from the GC increases. Hence, one would expect to have maximum yield from the GC survey when the screen is far enough from the GC and the survey is at a high frequency. These aforementioned effects help us in constraining the optimum frequency for future GC surveys. Note that the optimum frequency largely depends on the bandwidth of the survey if it is backend limited. The 2-D histograms also suggest that the optimum frequency for future GBT surveys is as high as 9 GHz for CPs and 22 GHz for MSPs for strong and weak scattering cases if we assume the backends can cover the whole bandwidth of the receiver. On the other hand, if we consider VEGAS as the backend for future surveys, we obtain an optimum frequency of ∼9 GHz for CPs for both, the strong and the weak scattering case. For MSPs, the optimum frequency is 22 GHz for the weak and strong scattering case. Since we are interested in finding CPs and MSPs, based on these results, we propose that the optimal range of frequencies for future GBT surveys is 9–14 GHz. We also note that future surveys of the GC in the range of 1.4–6 GHz will not be able to detect MSPs, not because of absorption but the faintness of the sources. In any case, we have to go to higher frequencies (> 9 GHz) to detect any pulsars in the GC in single observational tracks.

The results suggest that it would be more difficult to detect MSPs than CPs given the lower radio luminosities and the effect scattering has on their radio flux densities. We cannot favour any population at the moment because the analysis suggests that previous surveys have not been sensitive to any of the populations so far, even without factoring in the sources of flux density mitigation. Our conclusions differ from Macquart & Kanekar (2015), which can be attributed to the fact that the population used by (Macquart & Kanekar 2015) is the actual pulsar population, which might have an inherent selection bias in the pseudo-luminosity function of the source population as only the brightest pulsars have been detected by current radio telescopes. Hence, we sample only the tail of the underlying pseudo-luminosity distribution of pulsars, which can lead to different inferences about the source population. On the other hand, we have considered a synthetic population of pulsars in the GC, assuming an underlying pseudo-luminosity function, which properly accounts for this selection bias.

Recent results suggest that scattering does not play an important role in the attenuation of flux densities towards the GC. This is an important result for future surveys of the GC. If the weak scattering scenario is true then Fig. 1 suggests that deeper searches of the GC without going to higher and higher frequencies would result in more detections of pulsars. Future telescopes like the SKA and next generation Very Large Array (ngVLA) (Hughes et al. 2015) will provide a great opportunity to search for radio pulsars in the GC. These surveys are expected to detect significant fraction of the pulsar population in the inner Galaxy. Future high frequency radio surveys with highly sensitive radio telescopes will help in resolving the pulsar problem in the GC.

4 CONCLUSIONS

In summary, from an analysis of the current observational constraints of the pulsar population in the GC, our main conclusions are as follows: (i) the null results from previous surveys are not surprising, given that current surveys have only probed $\sim 2\%$ of the total CP population and 0% of the MSP population; (ii) upper limits on the CP and MSP population for various models constrain the population of pulsars beaming towards us to be < 445 CPs and < 5800 MSPs; (iii) a future GC survey with the GBT would have greater prospects of detecting CPs compared to MSPs. We find that the optimum frequency of a GBT survey would be 9–14 GHz; (iv) a future surveys with SKA-MID and ngVLA would probe a sizable population of the pulsar population in the GC.

ACKNOWLEDGEMENTS

We thank our anonymous referee for suggestions that vastly improved the manuscript. This research was partially supported by the National Science Foundation under Award No. OIA-1458952. Any opinions, findings and conclusions, or recommendations expressed in this material are those of the authors and do not necessarily reflect the views of the National Science Foundation.

APPENDIX A: CALCULATING REDUCTION IN FLUX DUE TO SCATTERING

Here, we describe the method to calculate the reduction in flux due to scattering. Since pulsar surveys make use of harmonic summing to increase the signal to noise of the detection in the Fourier domain, for each of previous and future survey, we find the optimum number of harmonics to be summed. For any survey, we follow the terminology in Cordes & Lazio (1997) and define the "pulsed fraction"

$$\eta_p = \sum_{0}^{N_h} \frac{R_l}{\sqrt{N_h}}, \tag{A1}$$

where N_h is the number of harmonics to be summed and

$$R_l = \frac{S(l)}{S(0)} \tag{A2}$$

is the ratio of the amplitude of the l^{th} harmonic and the amplitude of the DC component in the Fourier domain. For this analysis, we assume a Gaussian pulse characterized by

$$f_1(t) = \frac{1}{\sqrt{2\pi}\sigma} \exp\left[\frac{-t^2}{2\sigma^2}\right], \tag{A3}$$

where σ is the standard deviation and in our case, t is time running over one pulse period, P. For the scattered case, we convolve the Gaussian with a one-sided exponential function

with a mean of τ_s. This results in a modified pulse profile described by

$$f_2(t) = \frac{\lambda}{2}\ \exp\left(\sigma^2\lambda - 2t\right)\ \mathrm{erfc}\left(\sigma^2\lambda - t\right), \qquad \text{(A4)}$$

where $\lambda = 1/\tau_s$ and σ is the standard deviation of the Gaussian distribution and the complimentary error function

$$\mathrm{erfc}(x) = \frac{2}{\sqrt{\pi}}\int_x^\infty e^{-y^2}dy. \qquad \text{(A5)}$$

The scattering broadening function in time domain is given by,

$$f_{sca}(t) = \exp\left(-\frac{t}{\tau_s}\right). \qquad \text{(A6)}$$

In Fourier space, where the frequency of the l^{th} harmonic $k = l/P$, the Gaussian pulse transforms to

$$S_{\mathrm{Gauss}}(k) = \frac{1}{\sqrt{2\pi}}\exp\left(-\frac{\sigma^2k^2}{2}\right) \qquad \text{(A7)}$$

and the scatter broadening function transforms to

$$S_{\mathrm{sca}}(k) = \frac{1}{(k^2\tau_s^2 + 1)}. \qquad \text{(A8)}$$

The resulting Fourier components are then

$$S(k) = S_{\mathrm{Gauss}}(k)\cdot S_{\mathrm{sca}}(k). \qquad \text{(A9)}$$

$f_1(t)$ and $f_2(t)$ reported here are already normalized to make sure that the area under the pulse within one pulse period is the same for both functions. After normalizing the pulse from both scenarios, we computed the Fourier transform for the standard and scattered pulse.

Then, we obtained the optimal number of harmonics to be summed and computed the pulsed fraction using Eq. A1. The optimum number of harmonics to be summed will be the value N_h for which Eq. A1 is maximized. Figure. A1 shows one such result for a strong scattering scenario for CPs for a fixed duty cycle. In the case of strong scattering, the value of N_h is lower and the maximum value of the pulsed fraction is significantly lower than the unscattered case. This means that the sensitivity of the survey reduces by a factor of the ratio of the two pulsed fractions,

$$\mathcal{S}(\nu) = \frac{\eta_{p,g}}{\eta_{p,sca}}. \qquad \text{(A10)}$$

REFERENCES

Bailes M., Johnston S., Bell J. F., Lorimer D. R., Stappers B. W., Manchester R. N., Lyne A. G., Nicastro L., Gaensler B. M., 1997, ApJ, 481, 386

Bates S. D., Johnston S., Lorimer D. R., Kramer M., Possenti A., Burgay M., Stappers B., Keith M. J., Lyne A., Bailes M., McLaughlin M. A., O'Brien J. T., Hobbs G., 2011, MNRAS, 411, 1575

Bates S. D., Lorimer D. R., Rane A., Swiggum J., 2014, MNRAS, 439, 2893

Bates S. D., Lorimer D. R., Verbiest J. P. W., 2013, MNRAS, 431, 1352

Bower G. C., Deller A., Demorest P., Brunthaler A., Eatough R., Falcke H., Kramer M., Lee K. J., Spitler L., 2014, ApJL, 780, L2

Burgay M., Bailes M., Bates S. D., Bhat N. D. R., Burke-Spolaor S., Champion D. J., Coster P., D'Amico N., et al. 2013, MNRAS, 433, 259

Bussa S., VEGAS Development Team 2012, in American Astronomical Society Meeting Abstracts #219 Vol. 219 of American Astronomical Society Meeting Abstracts, VEGAS: VErsatile GBT Astronomical Spectrometer. p. 446.10

Carilli C. L., McKinnon M., Ott J., Beasley A., Isella A., Murphy E., Leroy A., Casey C., et al. 2015, ArXiv e-prints 1510.06438

Chennamangalam J., Lorimer D. R., 2014, MNRAS, 440, L86

Cordes J. M., Chernoff D. F., 1997, ApJ, 482, 971

Cordes J. M., Lazio T. J. W., 1997, ApJ, 475, 557

Deneva I. S., 2010, PhD thesis, Cornell University

Dexter J., O'Leary R. M., 2014, ApJL, 783, L7

Eatough R., Karuppusamy R., Kramer M., Klein B., Champion D., Kraus A., Keane E., Bassa C., Lyne A., Lazarus P., Verbiest J., Freire P., Brunthaler A., Falcke H., 2013, The Astronomer's Telegram, 5040

Edwards R. T., Bailes M., van Straten W., Britton M. C., 2001, MNRAS, 326, 358

Faucher-Giguère C.-A., Kaspi V. M., 2006, ApJ, 643, 332

Genzel R., Eisenhauer F., Gillessen S., 2010, Reviews of Modern Physics, 82, 3121

Gillessen S., Genzel R., Fritz T. K., Quataert E., Alig C., Burkert A., Cuadra J., Eisenhauer F., Pfuhl O., Dodds-Eden K., Gammie C. F., Ott T., 2012, Nature, 481, 51

Hooper D., Linden T., 2016, JCAP, 8, 018

Hughes A. M., Beasley A., Carilli C., 2015, IAU General Assembly, 22, 2255106

Johnston S., Kramer M., Lorimer D. R., Lyne A. G., McLaughlin M., Klein B., Manchester R. N., 2006, MNRAS, 373, L6

Kijak J., Gupta Y., Krzeszowski K., 2007, A&A, 462, 699

Kijak J., Lewandowski W., Maron O., Gupta Y., Jessner A., 2011, A&A, 531, A16

Krishnakumar M. A., Mitra D., Naidu A., Joshi B. C., Manoharan P. K., 2015, ApJ, 804, 23

Law C. J., Yusef-Zadeh F., Cotton W. D., Maddalena R. J., 2008, ApJS, 177, 255

Lewandowski W., Rożko K., Kijak J., Melikidze G. I., 2015, ApJ, 808, 18

Lorimer D. R., Esposito P., Manchester R. N., Possenti A., Lyne A. G., McLaughlin M. A., Kramer M., Hobbs G., Stairs I. H., Burgay M., Eatough R. P., Keith M. J., Faulkner A. J., D'Amico N., Camilo F., Corongiu A., Crawford F., 2015, MNRAS, 450, 2185

Lorimer D. R., Faulkner A. J., Lyne A. G., Manchester R. N., Kramer M., McLaughlin M. A., Hobbs G., Possenti A., Stairs I. H., Camilo F., Burgay M., D'Amico N., Corongiu A., Crawford F., 2006, MNRAS, 372, 777

Macquart J.-P., Kanekar N., 2015, ApJ, 805, 172

Macquart J.-P., Kanekar N., Frail D. A., Ransom S. M., 2010, ApJ, 715, 939

Manchester R. N., Lyne A. G., Camilo F., Bell J. F., Kaspi V. M., D'Amico N., McKay N. P. F., Crawford F., et al. 2001, MNRAS, 328, 17

Mori K., Gotthelf E. V., Zhang S., An H., Baganoff F. K., Barrière N. M., Beloborodov A. M., Boggs S. E., Christensen F. E. e. a., 2013, ApJL, 770, L23

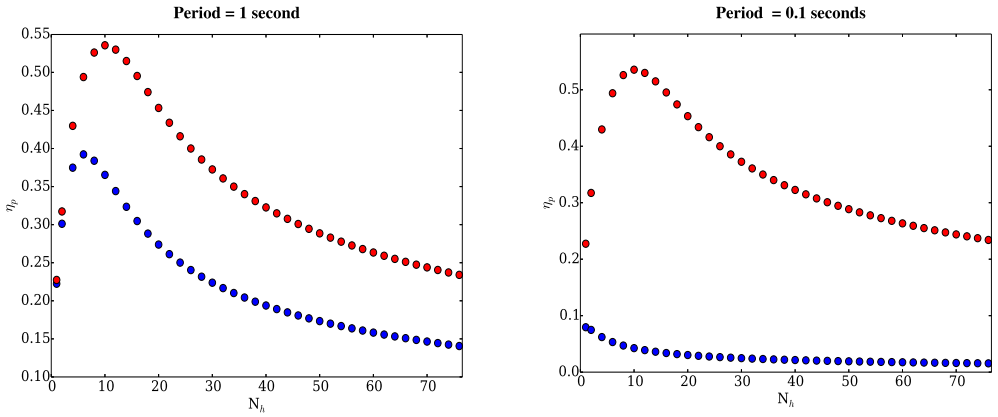

Figure A1. Pulsed fraction versus number of harmonics summed for a Gaussian pulse (red dots) and a scattered pulse (blue dots). We assume a constant duty cycle of 5%. We can see that smaller periods are severely affected by scattering.

Morris M., Serabyn E., 1996, ARAA, 34, 645

Pedlar A., Anantharamaiah K. R., Ekers R. D., Goss W. M., van Gorkom J. H., Schwarz U. J., Zhao J.-H., 1989, ApJ, 342, 769

Press W. H., Teukolsky S. A., Vetterling W. T., Flannery B. P., 2002, Numerical recipes in C++ : the art of scientific computing. Cambridge University Press

Rajwade K., Lorimer D. R., Anderson L. D., 2016, MNRAS, 455, 493

Ransom S. M., Demorest P., Ford J., McCullough R., Ray J., DuPlain R., Brandt P., 2009, in American Astronomical Society Meeting Abstracts #214 Vol. 214 of American Astronomical Society Meeting Abstracts, GUPPI: Green Bank Ultimate Pulsar Processing Instrument. p. 605.08

Schödel R., Eckart A., Alexander T., Merritt D., Genzel R., Sternberg A., Meyer L., Kul F., Moultaka J., Ott T., Straubmeier C., 2007, A&A, 469, 125

Sieber W., 1973, A& A, 28, 237

Wharton R. S., Chatterjee S., Cordes J. M., Deneva J. S., Lazio T. J. W., 2012, ApJ, 753, 108